



**AFRL-RZ-WP-TP-2012-0134**

**USE OF ULTRASONIC FORCE MICROSCOPY TO IMAGE  
THE INTERIOR NANOPARTICLES IN  $\text{YBa}_2\text{Cu}_3\text{O}_{7-x}$   
FILMS (POSTPRINT)**

**Chakrapani V. Varanasi, Vijay Nalladega, and S. Sathish**

**University of Dayton Research Institute**

**Timothy J. Haugan and Paul N. Barnes**

**Mechanical Energy Conversion Branch  
Energy/Power/Thermal Division**

**FEBRUARY 2012**

**Approved for public release; distribution unlimited.**

*See additional restrictions described on inside pages*

**STINFO COPY**

**© 2007 IEEE**

**AIR FORCE RESEARCH LABORATORY  
PROPULSION DIRECTORATE  
WRIGHT-PATTERSON AIR FORCE BASE, OH 45433-7251  
AIR FORCE MATERIEL COMMAND  
UNITED STATES AIR FORCE**

REPORT DOCUMENTATION PAGE				Form Approved OMB No. 0704-0188	
<p>The public reporting burden for this collection of information is estimated to average 1 hour per response, including the time for reviewing instructions, searching existing data sources, gathering and maintaining the data needed, and completing and reviewing the collection of information. Send comments regarding this burden estimate or any other aspect of this collection of information, including suggestions for reducing this burden, to Department of Defense, Washington Headquarters Services, Directorate for Information Operations and Reports (0704-0188), 1215 Jefferson Davis Highway, Suite 1204, Arlington, VA 22202-4302. Respondents should be aware that notwithstanding any other provision of law, no person shall be subject to any penalty for failing to comply with a collection of information if it does not display a currently valid OMB control number. <b>PLEASE DO NOT RETURN YOUR FORM TO THE ABOVE ADDRESS.</b></p>					
1. REPORT DATE (DD-MM-YY) February 2012		2. REPORT TYPE Journal Article Postprint		3. DATES COVERED (From - To) 04 April 2005 – 04 April 2007	
4. TITLE AND SUBTITLE USE OF ULTRASONIC FORCE MICROSCOPY TO IMAGE THE INTERIOR NANOPARTICLES IN YBa <sub>2</sub> Cu <sub>3</sub> O <sub>7-x</sub> FILMS (POSTPRINT)				5a. CONTRACT NUMBER In-house	
				5b. GRANT NUMBER	
				5c. PROGRAM ELEMENT NUMBER 62203F	
6. AUTHOR(S) Chakrapani V. Varanasi, Vijay Nalladega, and S. Sathish (University of Dayton Research Institute) Timothy J. Haugan and Paul N. Barnes (AFRL/RZPG)				5d. PROJECT NUMBER 3145	
				5e. TASK NUMBER 32	
				5f. WORK UNIT NUMBER 314532ZE	
7. PERFORMING ORGANIZATION NAME(S) AND ADDRESS(ES) University of Dayton Research Institute Dayton, OH 45469				8. PERFORMING ORGANIZATION REPORT NUMBER AFRL-RZ-WP-TP-2012-0134	
9. SPONSORING/MONITORING AGENCY NAME(S) AND ADDRESS(ES) Air Force Research Laboratory Propulsion Directorate Wright-Patterson Air Force Base, OH 45433-7251 Air Force Materiel Command United States Air Force				10. SPONSORING/MONITORING AGENCY ACRONYM(S) AFRL/RZPG	
				11. SPONSORING/MONITORING AGENCY REPORT NUMBER(S) AFRL-RZ-WP-TP-2012-0134	
12. DISTRIBUTION/AVAILABILITY STATEMENT Approved for public release; distribution unlimited.					
13. SUPPLEMENTARY NOTES Journal article published in <i>IEEE Transactions on Applied Superconductivity</i> , Vol. 17, No. 2, June 2007. © 2007 IEEE. The U.S. Government is joint author of this work and has the right to use, modify, reproduce, release, perform, display, or disclose the work. PA Case Number: AFRL/WS 07-0629; Clearance Date: 04 Apr 2007. Work on this effort was completed in 2007. Paper contains color content.					
14. ABSTRACT Nanoparticles present in the interior of YBa <sub>2</sub> Cu <sub>3</sub> O <sub>7-x</sub> (YBCO) films were successfully imaged for the first time by using an ultrasonic force microscope (UFM), which can also operate as a conventional atomic force microscope (AFM). Nanoparticles of Y <sub>2</sub> BaCuO <sub>5</sub> and BaSnO <sub>3</sub> were introduced into YBCO films using pulsed laser ablation to improve critical current density via enhanced flux pinning. The scanning speed and ultrasonic frequencies in the range of 300–500 kHz were optimized for each sample such that the nanometer sized particles on the surface as well as from the film interior can be imaged with good contrast and resolution. UFM and AFM scans taken of the same locations were compared to show the advantages of using UFM over AFM. We demonstrate that UFM can be used nondestructively to both characterize the interior nanoparticles introduced in YBCO films and provide high resolution images of the screw dislocation induced terraces present in the films.					
15. SUBJECT TERMS nanoparticles, interior, pulsed laser ablation, critical current density, ultrasonic, terraces, screw dislocation, frequencies					
16. SECURITY CLASSIFICATION OF:			17. LIMITATION OF ABSTRACT: SAR	18. NUMBER OF PAGES 10	19a. NAME OF RESPONSIBLE PERSON (Monitor) Timothy J. Haugan 19b. TELEPHONE NUMBER (Include Area Code) N/A
a. REPORT Unclassified	b. ABSTRACT Unclassified	c. THIS PAGE Unclassified			

# Use of Ultrasonic Force Microscopy to Image the Interior Nanoparticles in $\text{YBa}_2\text{Cu}_3\text{O}_{7-x}$ Films

Chakrapani V. Varanasi, Vijay Nalladega, S. Sathish, Timothy Haugan, and Paul N. Barnes

**Abstract**—Nanoparticles present in the interior of  $\text{YBa}_2\text{Cu}_3\text{O}_{7-x}$  (YBCO) films were successfully imaged for the first time by using an ultrasonic force microscope (UFM), which can also operate as a conventional atomic force microscope (AFM). Nanoparticles of  $\text{Y}_2\text{BaCuO}_5$  and  $\text{BaSnO}_3$  were introduced into YBCO films using pulsed laser ablation to improve critical current density via enhanced flux pinning. The scanning speed and ultrasonic frequencies in the range of 300–500 kHz were optimized for each sample such that the nanometer sized particles on the surface as well as from the film interior can be imaged with good contrast and resolution. UFM and AFM scans taken of the same locations were compared to show the advantages of using UFM over AFM. We demonstrate that UFM can be used nondestructively to both characterize the interior nanoparticles introduced in YBCO films and provide high resolution images of the screw dislocation induced terraces present in the films.

**Index Terms**—Fluxpinning, nanoparticles, nondestructive testing, ultrasonic force microscopy, YBCO coated conductors.

## I. INTRODUCTION

THE critical current density ( $J_c$ ) in applied magnetic fields of superconducting  $\text{YBa}_2\text{Cu}_3\text{O}_{7-x}$  (YBCO) coated conductors can be enhanced by incorporating a high density of defects that act as pinning centers for the fluxons penetrating the material at these fields. Pinning is effective when the defect size approaches the coherence length,  $\sim 2\text{--}4\text{ nm}$  for YBCO at 77 K [1]. It has been shown that by adding nonsuperconducting nanoparticles such as  $\text{Y}_2\text{BaCuO}_5$  (Y211),  $\text{BaZrO}_3$ , and  $\text{BaSnO}_3$  in pulsed laser deposited (PLD) YBCO films, the  $J_c$  of YBCO coatings can be significantly improved [2]–[8]. Other second phase particles such as  $\text{Y}_2\text{O}_3$  and  $(\text{Y}, \text{Sm})_2\text{O}_3$  were also introduced into YBCO deposited by other methods such as metal-organic deposition (MOD) and metallo-organic chemical vapor deposition (MOCVD) to improve the performance [9], [10]. In general, nanoparticles can pin the fluxons very effectively via collective pinning if the appropriate size and volumetric density are maintained. This method of second phase nanoparticulate additions is expected to be economical over other means of creating the defects such as ion irradiation [11], etc.

To optimize the YBCO coated conductor performance through the addition (irrespective of the deposition method) of nanoparticles, knowledge of the particle size and distribution in the YBCO coatings is important. This information is needed to correlate with the pinning properties and subsequently modify the process for further improvements. Since the particles in the coatings are very small ( $\sim 2\text{--}20\text{ nm}$  size), transmission electron microscopy (TEM) is generally used for characterization. Although the TEM images provide very useful information about the particles, this method of characterization is destructive in nature and involves careful, laborious sample preparation. High resolution scanning electron microscopy (SEM) is an alternative method that can be used to image the nanoparticles. With the recent advancements in field emission electron guns, lens detectors (e.g. Thru Lens Detectors), etc., images with nanometer scale resolutions are routinely obtained using high resolution SEMs (e.g. SIRION). However, the SEM characterization also needs sample preparation that is destructive in nature by either applying conductive coatings onto the YBCO films or slicing the film to characterize the interior particles in cross-sectional images. Both of these methods take several days to determine the information about the particle size and distribution in the superconductors.

A nondestructive technique, such as an ultrasonic force microscope (UFM) can be very useful for the development of HTS coated conductor if it can be used to image the nanoparticles from the interior of the sample quickly. Ultrasonic force microscopy (UFM) has been demonstrated as a quick, nondestructive technique to image the internal microcracks and structural defects present in other material system [12], [13]. However, UFM has not been used to image the particles present in YBCO superconductors before. Since the image contrast is created by the differences in the elastic modulus, it could be possible to image second-phase particles embedded in a matrix of different contrast, such as the nanometer-sized, material inclusions intentionally added to high temperature superconductors (HTS). While a conventional atomic force microscope (AFM) gives only topographical information, the UFM is capable of also imaging the defects from the interior of the sample.

The UFM measures the surface displacements caused by an acoustic wave that travels through the thickness of the sample and forms the image depending upon the differences in the amplitude of the vibrations which is related to the stiffness of the material. It has been found that in many materials, even if contrast is poor in AFM images, the elastic property variations imaged in UFM enhances the contrast [14], [15]. This particularly becomes useful when the surface topography variations imaged in AFM is extremely low. As an example, internal micro-cracks

Manuscript received August 25, 2006. The Air Force Office of Scientific Research and the Propulsion Directorate of the Air Force Research Laboratory supported this work.

C. V. Varanasi, V. Nalladega, and S. Sathish are with the University of Dayton Research Institute, Dayton, OH 45469 USA (e-mail: chakrapani.varanasi@wpafb.af.mil).

T. Haugan and P. N. Barnes are with the Air Force Research Laboratory, Propulsion Directorate, Wright-Patterson AFB, OH 45433 USA.

Color versions of one or more of the figures in this paper are available online at <http://ieeexplore.ieee.org>.

Digital Object Identifier 10.1109/TASC.2007.897920

in an  $\text{Al}_2\text{O}_3$  –  $\text{TiC}$  composite can be imaged as a distinctive crack with UFM when not visible with AFM [14]. The free boundary at the crack contributes more contrast due to the increased amplitude of the acoustic wave in the immediate vicinity of the crack. On the basis of same principle, UFM can also be used to detect interface delaminations [13], [16] in multilayer samples.

With the differences in elastic modulus, it is quite plausible for UFM to image any second phase particles embedded in the matrix with a different contrast, resulting in an image that distinguishes particles from the matrix. When optimized, this method gives the opportunity to image the defects in coatings in thickness of 100 nm [17] or more. The depth of defect detection depends on the applied force and the probing tip radius of curvature. For thin film HTS superconductor samples with a thickness of  $\sim 300$  nm, a sampling depth of 100 nm range gives most of the bulk information and would be reasonable to image by UFM the imbedded, nanometer-sized, material inclusions. As a quick, nondestructive characterization tool, UFM may be a highly desirable alternative for 3-D characterization of the pinning centers in superconducting thin films. In this report, the initial results are presented of using an UFM to image the interior nanoparticles present in YBCO coatings.

## II. EXPERIMENTAL

All the YBCO coating samples in the present work with nanoparticles were prepared by pulsed laser ablation using a 248 nm KrF excimer laser (Lambda Physik). A special target was made with a  $\text{BaSnO}_3$  sector placed on a YBCO target. Such a dual phase sector target was successfully used to introduce nanoparticles of  $\text{Y}_2\text{BaCuO}_5$  (Y211) in YBCO coatings as discussed in detail elsewhere [2]. As the target is rotated each sector is ablated periodically causing the formation of nanoparticles in the matrix. Single crystal (100)  $\text{LaAlO}_3$  substrates were used for the deposition of the YBCO +  $\text{BaSnO}_3$  composite coatings which had a thickness of  $\sim 350$  nm. The magnetization critical current density ( $J_{\text{cm}}$ ) of the YBCO +  $\text{BaSnO}_3$  samples were obtained at 77 K using a vibrating sample magnetometer (Quantum Design PPMS) and compared with a typical YBCO sample. To demonstrate material diversity for the UFM, additional samples were deposited by PLD using a technique where two separate Y211 and YBCO targets were alternated during the ablation to create the particulate dispersion. This resulted in a multilayered sample where the Y211 nanoparticles were sandwiched between nanolayers of YBCO [3]. In this particular sample, the layers were terminated with a final Y211 nanoparticle layer. The total thickness of the film in this sample was  $\sim 290$  nm.

YBCO coated conductor samples were also prepared for imaging by UFM. Biaxially textured Ni-5 at %W substrates were buffered with layers of  $\text{CeO}_2$ , yttria-stabilized zirconia (YSZ), and  $\text{CeO}_2$  in that order by pulsed laser ablation. A final YBCO layer was then grown on the buffer layers. The deposition conditions used for the various layers are discussed elsewhere [18]. The total thickness of both  $\text{CeO}_2$  layers was  $\sim 50$  nm, YSZ was  $\sim 500$  nm, and the YBCO layer was  $\sim 300$  nm.

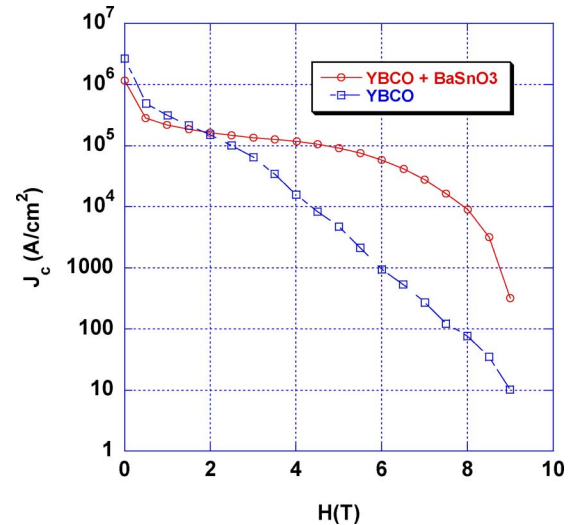


Fig. 1. Magnetization  $J_c$  data of YBCO and YBCO +  $\text{BaSnO}_3$  samples measured at 77 K.

A Digital Instruments Dimension 3000 Nanoscope III AFM has been modified in house to operate as an UFM. Specific details of the instrument used in the present study are discussed elsewhere [14]. Briefly, to perform UFM imaging, an ultrasonic transducer operating in the frequency range of few hundred KHz to 1 MHz is attached to the bottom of the sample. The top surface of the sample is in contact with an AFM tip. The AFM is operated in standard contact mode and both AFM and UFM images are acquired of the same location. To optimize the conditions for UFM imaging, a good AFM image is first obtained and then the frequency and amplitude of acoustic excitation are optimized to obtain a clear UFM image. The images presented in this paper were obtained with silicon nitride cantilevers with a low spring constant ( $k_c = 0.12$  N/m). YBCO coatings on (100)  $\text{LaAlO}_3$  and multilayered buffered metallic substrates processed with different nanoparticles ( $\text{BaSnO}_3$ ,  $\text{Y}_2\text{BaCuO}_5$ ) were characterized. The scan speed and ultrasonic frequency (100-500 KHz) were optimized to image the internal nanometer-sized particles as well as the particles on the surface. SIRION high resolution SEM was also used to analyse the samples for comparison to the data obtained by using the UFM.

## III. RESULTS AND DISCUSSION

Fig. 1 shows the magnetization critical current density ( $J_{\text{cm}}$ ) data of the YBCO +  $\text{BaSnO}_3$  film sample compared with that of a typical YBCO film. The improvement in  $J_c$  in YBCO +  $\text{BaSnO}_3$  film was found to be more than an order of magnitude, especially at higher fields, indicating that improved flux pinning in these samples. More details on the flux pinning improvements are discussed elsewhere [7].

Figs. 2(a) and 2(b) show an AFM and an UFM image, respectively, taken of a YBCO film prepared with  $\text{BaSnO}_3$  nanoparticles. The UFM scan shows nanometer-sized particles from the interior as well as on the surface with high contrast compared to the YBCO matrix. The presence of such nanoparticles was verified by doing plan view SEM and TEM on similarly processed 2 samples. The composition of these particles was found to be rich

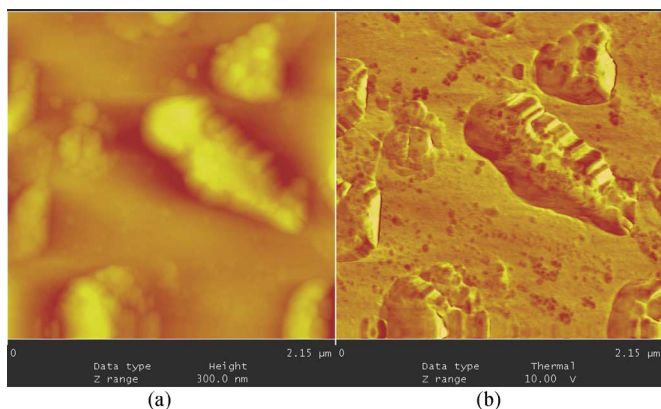


Fig. 2. (a) AFM surface topography image and (b) UFM image of a YBCO + BaSnO<sub>3</sub> coating sample. A frequency of 225 KHz and a scan rate of 1Hz were used to generate the UFM image. Image size is approximately 2 × 2 microns.

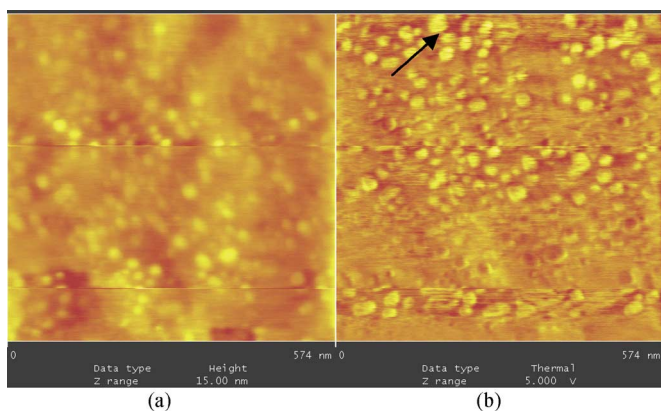


Fig. 3. (a) AFM surface topography image and (b) UFM image of YBCO sample with multiple layers of nm sized Y211 particles and YBCO on LaAlO<sub>3</sub> substrate. A frequency 117 KHz and a scan rate of 1 Hz were used to obtain this UFM image. One of the subsurface particles present in the image is identified.

in Ba and Sn (presumably BaSnO<sub>3</sub>) by performing energy dispersive x-ray analyses. The contrast differences in the UFM images observed is likely due to the difference in stiffness between the YBCO and BaSnO<sub>3</sub> materials. The location of the image was chosen due to the cluster of particles periodically found on the surface of PLD films for contrast comparison. The presence of such BaSnO<sub>3</sub> nanoparticles is believed to be responsible for observed flux pinning enhancement.

Fig. 3(b) shows an UFM image acquired on the Y211 pinned YBCO sample deposited on a (100) LaAlO<sub>3</sub> single crystal substrate and for comparison the AFM image (Fig. 3(a)) of the same location. It can be seen that in the UFM image, the nanometer sized Y211 particles (verified to be Y211 by TEM analyses) on the surface appear with good contrast compared to the AFM image. Additionally, internal Y211 particles of nanometer size were also detected in the UFM image again due to differences in stiffness between YBCO and Y211. One of them is indicated by an arrow. In the current UFM images, Y211 nanoparticles from the inside of the film are projected onto a two-dimensional surface.

Fig. 4 shows AFM and UFM images of YBCO coated conductor sample prepared with multiple buffer layers of CeO<sub>2</sub>, 3

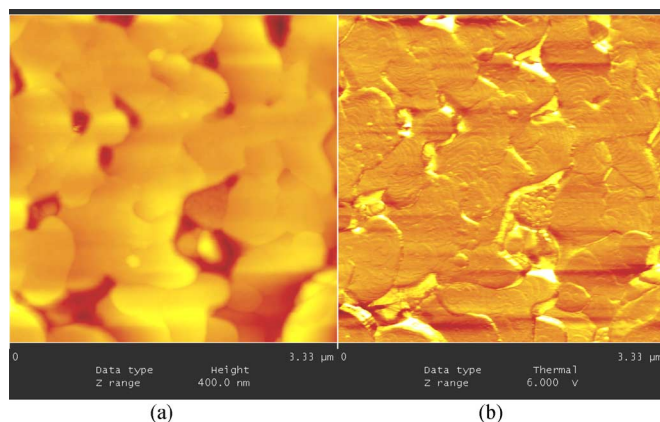


Fig. 4. (a) AFM surface topography and (b) UFM image of YBCO coated conductor sample with random Y211 particles and with a stack of CeO<sub>2</sub>, YSZ, CeO<sub>2</sub>, and buffer layers on a biaxially textured Ni-5 at %W substrate. The UFM images were obtained at an acoustic excitation frequency of 450 KHz and a scan rate of 1 Hz.

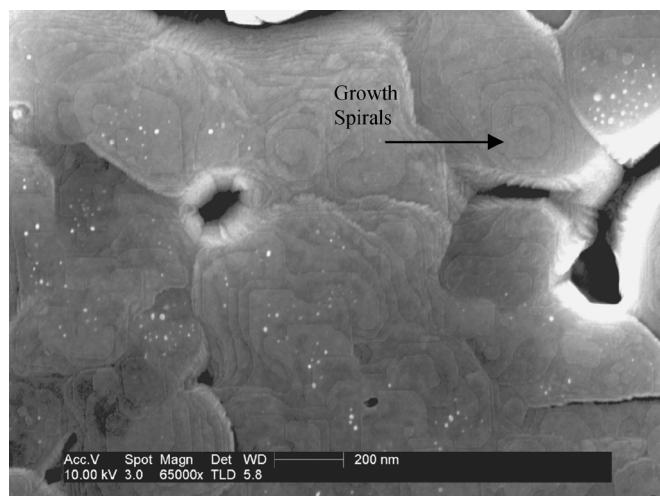


Fig. 5. High-resolution Scanning Electron Micrograph (SEM) showing the growth spirals in YBCO grains of a coated conductor sample. This image was taken using a high resolution SIRION microscope with thru lens detector (TLD).

yttria stabilized zirconia (YSZ), CeO<sub>2</sub> and YBCO on a biaxially textured Ni-5 at %W substrate. In the UFM image, Fig. 4(b), of this particular sample, the growth spirals present in individual grains can be seen clearly. With the UFM, such a high resolution images resolving the terraces of the spirals present in the grains were not achieved previously. In the standard AFM image, Fig. 4(a), such spirals were not typically observed. Fig. 5 shows a high resolution SEM picture of a similar sample (PLD deposited YBCO coating on CeO<sub>2</sub>/YSZ/CeO<sub>2</sub> buffered Ni-5at.%W) showing the spirals/terraces as observed in UFM. This confirms that the spirals imaged with the UFM are indeed the surface terraces. It can also be seen that there are some fine nanoparticles sparsely scattered in these samples. The SEM image was taken using a high resolution SIRION microscope using thru lens detectors (TLD) which made it possible to image these particles. This information was readily obtained by using an UFM in air with minimal sample preparation.



## IV. CONCLUSIONS

UFM was successfully used to image the nm-sized particles and growth spirals in the YBCO films. Nanoparticles of  $\text{BaSnO}_3$  and Y211 that were present on the surface as well as in the interior were imaged simultaneously with good contrast. The initial results presented here demonstrates the capability of the UFM to accomplish this and that improvements can now be considered to extend the imaging to graphically present 3-D images with multiple varied scans and appropriately developed software. Of particular interest is that UFM is nondestructive in nature, does not need extensive sample preparation, and its imaging can be performed in ambient air. Since UFM is a nondestructive technique, samples can be reused for further characterization of the same sample. This will allow for rapid process optimization to obtain the desired size and distribution of the nanoparticles.

## ACKNOWLEDGMENT

The authors acknowledge L. Brunke, J. Murphy, J. Burke, and I. Maartense of the University of Dayton Research Institute for sample preparation and for  $T_c$  measurements, and E. Stinzianni and K. Dunn of the College of Nanoscale Science and Engineering, University of Albany–State University of New York for the TEM work.

## REFERENCES

- [1] D. Larbalestier, A. Gurevich, D. M. Feldmann, and A. Polyanskii, "High- $T_c$  superconducting materials for electric power applications," *Nature*, vol. 414, pp. 368–377, 2001.
- [2] C. Varanasi, P. N. Barnes, J. Burke, J. Carpenter, and T. J. Haugan, "Controlled introduction of flux pinning centers in  $\text{YBa}_2\text{Cu}_3\text{O}_{7-x}$  films during pulsed-laser deposition," *Appl. Phys. Lett.*, vol. 87, pp. 262510–262512, 2005.
- [3] T. J. Haugan, P. N. Barnes, R. Wheeler, F. Meisenkothen, and M. Sumption, "Addition of nanoparticle dispersions to enhance flux pinning of the  $\text{YBa}_2\text{Cu}_3\text{O}_{7-x}$  superconductor," *Nature*, vol. 430, pp. 867–870, 2004.
- [4] J. L. MacManus-Driscoll, S. R. Foltyn, Q. X. Jia, H. Wang, A. Serquis, L. Civale, B. Maiorov, M. E. Hawley, M. P. Maley, and D. E. Peterson, "Strongly enhanced current densities in superconducting coated conductors of  $\text{YBa}_2\text{Cu}_3\text{O}_{7-x} + \text{BaZrO}_3$ ," *Nature Materials*, vol. 3, pp. 439–441, 2004.
- [5] J. M. Huijbregtse, B. Dam, R. C. F. van der Geest, F. C. Klaassen, R. Elberse, J. H. Rector, and R. Griessen, "Natural strong pinning sites in laser-ablated  $\text{YBa}_2\text{Cu}_3\text{O}_{7-d}$  thin films," *Phys. Rev. B*, vol. 62, no. 2, p. 1338, 2000.
- [6] A. Goyal, S. Kang, K. J. Leonard, P. M. Martin, A. A. Gapud, M. Varela, M. Paranthaman, A. O. Ijaluola, E. D. Specht, J. R. Thomson, D. K. Christen, S. J. Pennycook, and F. A. List, "Irradiation-free columnar defects comprised of self assembled nanodots and nanorods resulting in strongly enhanced flux-pinning in  $\text{YBa}_2\text{Cu}_3\text{O}_{7-d}$  films," *Supercond. Sci. Technol.*, vol. 18, pp. 1533–1538, 2005.
- [7] C. V. Varanasi, P. N. Barnes, J. Burke, L. Brunke, I. Maartense, T. J. Haugan, E. A. Stinzianni, K. A. Dunn, and P. Haldar, "Flux pinning enhancement in  $\text{YBa}_2\text{Cu}_3\text{O}_{7-x}$  films with  $\text{BaSnO}_3$  nanoparticles," *Supercond. Sci. Technol.*, vol. 19, pp. L37–L41, 2006.
- [8] J. Hanisch, C. Cai, R. Huhne, L. Schulz, and B. Holzapfel, "Formation of nano-sized  $\text{BaIrO}_3$  precipitates and their contribution to flux pinning in Ir-doped  $\text{YBa}_2\text{Cu}_3\text{O}_{7-d}$  quasi-multilayers," *Appl. Phys. Lett.*, vol. 86, pp. 122508–122510, 2005.
- [9] U. Schoop, M. W. Rupich, C. Thieme, D. T. Verebelyi, W. Zhang, X. Li, T. Kodenkandath, N. Nguyen, E. Siegal, L. Civale, T. Holesinger, B. Maiorov, A. Goyal, and M. Paranthaman, "Second generation HTS wire based on RABiTS substrates and MOD YBCO," *IEEE Trans. on Appl. Supercond.*, vol. 15, no. 2, p. 2611, 2005.
- [10] X. Song, Z. Chen, S.-I. Kim, D. M. Feldman, D. Larbalestier, J. Reeves, Y. Xie, and V. Selvamanickam, "Evidence for strong flux pinning by small dense nanoprecipitates in a Sm-doped  $\text{YBa}_2\text{Cu}_3\text{O}_{7-d}$  coated conductor," *Appl. Phys. Lett.*, vol. 88, p. 21508, 2006.
- [11] L. Civale, "Vortex pinning and creep in superconductors with columnar defects," *Supercond. Sci. Technol.*, vol. 10, pp. A11–A28, 1997.
- [12] T. Tsuji and K. Yamanaka, "Observation by ultrasonic atomic force microscopy of reversible displacement of subsurface dislocations in highly oriented pyrolytic graphite," *Nanotechnology*, vol. 12, p. 301, 2001.
- [13] A. P. McGuigan, B. D. Huey, G. A. D. Briggs, O. V. Kolosov, Y. Tsukahara, and M. Yanaka, "Measurement of debonding in cracked nanocomposites films by ultrasonic force microscopy," *Appl. Phys. Lett.*, vol. 80, p. 1180, 2000.
- [14] K. Yamanaka, H. Ogiso, and O. Kolosov, "Ultrasonic force microscopy for nanometer resolution subsurface imaging," *Appl. Phys. Lett.*, vol. 64, p. 178, 1994.
- [15] C. Druffner and S. Sathish, "Atomic force and ultrasonic force microscopic investigation of laser treated ceramic head sliders," *J. Am. Ceram. Soc.*, vol. 86, p. 2122, 2003.
- [16] V. Nalladege, S. Sathish, and A. Brar, "Non-destructive evaluation of sub-micron delaminations at polymer/metal interface in flex circuits," in *Proceedings of the QNDE Conference*, Brunswick, Maine, July 31–August 5 2005, submitted for publication.
- [17] A. F. Sarioglu, A. Atalar, and F. L. Degertekin, "Modeling the effect of subsurface interface defects on contact stiffness for ultrasonic atomic force microscopy," *Appl. Phys. Lett.*, vol. 84, p. 5368, 2004.
- [18] P. N. Barnes, R. M. Nekkanti, T. J. Haugan, T. A. Campbell, N. A. Yust, and J. M. Evans, "Pulsed laser deposition of YBCO coated conductor using  $\text{Y}_2\text{O}_3$  as the seed and cap layer," *Supercond. Sci. Technol.*, vol. 17, pp. 957–962, 2004.